

Risk-Inspired Aerial Active Exploration for Enhancing Autonomous Driving of UGV in Unknown Off-Road Environments

Rongchuan Wang¹, Mengyin Fu^{1,2}, Jing Yu¹, Yi Yang¹, Wenjie Song^{1,*}

Abstract—Unknown area exploration is a crucial but challenging task for autonomous driving of unmanned ground vehicles (UGV) in unknown off-road environments. However, the exploration efficiency of a single UGV is low due to its limited sensing range. To solve this problem, this paper proposes a risk-inspired aerial active exploration system, which utilizes the flexibility and field of view advantages of Unmanned Aerial Vehicles (UAV) to guide the UGV in unknown off-road environments. Firstly, a fast terrain risk mapping method that can be used for both UAV and UGV is developed. This method efficiently combines quadtree and hash table data structure to enable UAV to analyze large scale terrain point cloud in real time. Based on the risk mapping result, a risk-inspired active exploration method is proposed to actively search a safe reference path for the UGV, which introduces terrain risk information into the process of travel point selection. Finally, the reference path is gradually generated and optimized, so that the UGV can safely and smoothly follow the path to the target location. Compared with single UGV exploration system, our approach reduces the overall path risk by 26.8% in simulated experiments, showing that the proposed system can enhance autonomous driving of the UGV and help it effectively avoid high-risk areas in unknown off-road environments.

I. INTRODUCTION

Unmanned ground vehicles (UGV) have been widely used in search and rescue tasks in unknown off-road environments. These tasks often require the UGV to autonomously navigate to the target location both safely and as quickly as possible [1]. However, prior road information is usually unavailable in unknown off-road environments, which makes it impossible to obtain a global path for the UGV in advance [2]. In this case, the UGV can only search for path by autonomous exploration to complete the navigation task. However, due to the low angle of view and limited field of view, the path exploration range of single UGV is small. Furthermore, body bumps caused by the fluctuating terrain bring large uncertainties to the sensor measurements of the UGV, and the randomly distributed obstacles seriously obscure the sensing field of the UGV, which both reduce the exploration efficiency. Therefore,

This work was partly supported by Program for National Natural Science Foundation of China (Grant No. 62373052, U1913203 and 61973034), Youth Talent Promotion project of China Association for science and technology, Beijing Institute of Technology Research Fund Program for Young Scholars.

¹The authors are with the School of Automation, Beijing Institute of Technology, Beijing 100081, P.R.China.

²The author is also with Nanjing University of Science and Technology, Nanjing 210014, P.R.China.

*Corresponding author: Wenjie Song (email: songwj@bit.edu.cn).

to enhance the path exploration ability is a key problem for the UGV in unknown off-road environments.

In order to solve this problem, many researchers consider deploying multi-robot systems including both Unmanned aerial vehicles (UAV) and UGV, which utilize the stronger flexibility and broader sensing range of the UAV to help the UGV find feasible path in unknown environments [3]–[6], [8]. For example, some researchers used an UAV to exhaustively explore the unknown area by remote control or autonomous exploration to establish a prebuilt map, and the global path for the UGV was generated based on the map [3]. Although this method can obtain prior information, the system relies on several assumptions and is not suitable for real-time tasks like rescue. Some other researches focused on sharing local sensing results of different robots in real time to improve the exploration process [5] [6]. Kulkarni et al. [6] periodically fused local voxel maps of an UAV and a legged robot to update their navigation graphs in an unknown mine, which enabled the legged robot to autonomously explore the area. This kind of scheme has good time efficiency during exploration, but it requires large and stable communication bandwidth which are difficult to achieve in unknown off-road environments. In addition, some other studies directly extracted path for the UGV instantaneously by aerial exploration, which did not bring heavy communication burden [8]. The path extracted by the UAV can provide a general reference for the UGV to avoid traps and reduce the exploration time cost.

Inspired by the above analysis, based on our previous work [7] where cross-view terrain point clouds measured from UAV and UGV are accurately matched and fused with terrain risk features, we further propose an active path finding system for the UGV assisted by an UAV in large unknown off-road environments. The main contributions are listed as follows:

- A risk-inspired aerial active exploration system is developed, where the UAV can simultaneously explore the unknown off-road environment and build large-scale terrain risk maps to generate a safe and efficient reference path for the UGV. With the reference path, the UGV can reduce reentries and avoid high-risk areas, enhancing the efficiency of UGV's autonomous driving in unknown off-road environments.
- A simulated large-scale off-road environment model is built to analyze the performance of the proposed system in detail. Several tests are conducted in the simulated

environment, where both quantitative and qualitative results can demonstrate the effectiveness and utility of our system.

II. RELATED WORK

A. Active Exploration

The existing approaches of robot active exploration can be generally divided into two categories: sampling-based approaches and frontier-based approaches. For sampling-based approaches, viewpoints are usually sampled randomly with the robot sensing range and selected as the local goals by calculating their contributions to the task [9]–[13]. For example, Cao et al. [9] uniformly sample a set of viewpoint candidates from a lattice pattern and define the uncovered space as the reward of each viewpoint to enable the ground robot to explore the unknown environment. In [11], the authors design a hierarchical gain to distinguish the priority of the uniformly sampled viewpoints for active 3D reconstruction tasks. However, the sampling-based approaches often require large computational cost to maintain the sampling space and contribution calculation, which may reduce the overall efficiency.

The frontier-based approach was first introduced in [14]. The main step of this approach is frontier detection, which is the boundary between the open and unknown space of the robot map, and many researchers have developed a variety of frontier detection methods [8], [14]–[18]. In [14], a naive frontier detection approach was proposed to conduct frontier detection on the entire map, which was time-consuming in large environment. To speed up the detection process, wavefront frontier detector (WFD) and fast frontier detector (FFD) were designed by Keidar and Kaminka [15]. This kind of method limits the detection area to the newly observed space of the map, which significantly improves the computation efficiency. Best et al. [18] designed different frontier detection methods for the maps generated by vision and range sensors respectively, which are also applied to a multi-robot cooperative system to obtain good exploration performance. Considering the real-time requirement of rescue mission, Zhang et al. [8] designed a unique cost function to select target point after frontier detection in their aerial-ground system. This method can enable the UGV to reach the goal quickly in the unknown environment, but it lacks consideration of terrain risk information which is necessary in off-road environments.

Inspired by [8], we develop a frontier-based exploration approach on the UAV. A multi-factor cost function is designed to incorporate terrain risk information into priority calculation of the local frontiers, which can ensure that the UAV can explore safe path for the UGV.

B. Air-Assisted Traversable Area Extraction

Nowadays, there are many researches related to traversable area extraction from the aerial measurements. Some researches mainly focused on directly extracting road from orthophoto images, such as RoadTracer proposed by Bastani et al. [19]

and D-Linknet proposed by Zhou et al. [20]. However, these approaches can not achieve good performance in off-road environments because the road characteristics are often not obvious on the complex terrain. Other researches attempted to extract traversable regions by training neural networks to deepen the understanding of terrain characteristics [21]–[23]. Although these methods can be effective in off-road environments, most of them have a strong dependence on training data, and data labeling in off-road environments is much more difficult.

There are also many researches focusing on extracting traversable regions from 3D point clouds. In [26], the researchers performed obstacle detection from 3D point cloud maps generated by monocular camera reconstruction. This approach is time consuming which is not suitable for real-time tasks. Russell et al. [27] equipped a DJI M600 with a rotating 16-line LiDAR for establishing terrain point clouds and extracting traversable areas from an aerial view, but the overall cost of the system is high. Moreover, some other researchers used lightweight depth cameras to extract the traversable area for unmanned vehicles in real time. For example, Fankhauser et al. [24] used a monocular depth camera to construct a 3D map to plan a path for legged robots. Kulkarni et al. [6] used a depth camera to construct and generate a plan graph. Path planning can be performed based on mapping results in these systems. However, due to the limited mapping range, the efficiency of them is low when applied to large scale off-road environment.

Our work is related to the 3D point cloud system. Specifically, considering the rapid development of solid-state lidar technology and its already good performance as in [25], we design a fast risk mapping method using a downward solid-state LiDAR on the UAV to perform real time terrain analysis in a large-scale off-road environment.

III. PROBLEM FORMULATION

A. Problem Statement

Let $Q \in \mathcal{R}^3$ be the unknown off-road environment. Define $\mathbf{p}_{\text{start}}, \mathbf{p}_{\text{end}} \in \mathcal{R}^2$ as the start and end points of the exploration task. Let M_g, M_d represent the local terrain analysis results of the UGV and UAV. Denote $\mathbf{p}_g, \mathbf{p}_d \in \mathcal{R}^2$ as the robots' 2D positions on xOy plane. Our problem can be defined as follows.

Problem: In an unknown off-road environment Q , given $M_g^{\text{current}}, M_d^{\text{current}}, \mathbf{p}_g^{\text{current}}, \mathbf{p}_d^{\text{current}}$, the UAV actively find a series of travel points $\mathbf{v}_k \{k = 1, 2, \dots, n\} \in \mathcal{R}^2$ to help the UGV generate a safe trajectory \mathbf{T}_g to move from $\mathbf{p}_{\text{start}}$ to \mathbf{p}_{end} as fast as possible.

B. System Overview

Our work mainly focuses on utilizing the broad sensing range and flexible traversability of the UAV to actively explore the unknown off-road environment and assist the UGV to complete navigation tasks safely and quickly. The main architecture of our system is shown in Fig. 1.

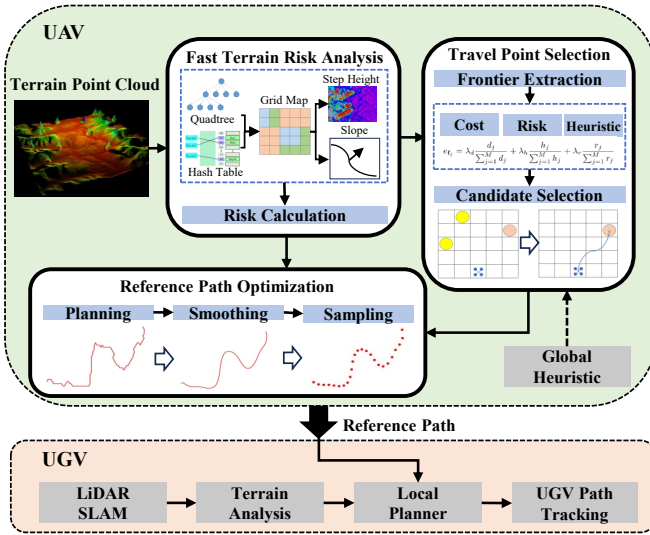


Fig. 1. The main architecture of the proposed system.

For the UAV, the flight altitude is set to a fixed value. Terrain point clouds are measured by a downward LiDAR and the local grid map is built and updated in real time. Then, a terrain analysis step is executed to get a top-view risk map from the grid map. The candidate frontiers are extracted from the top-view risk map. After that, the local travel point is scored and selected by a multi-factor cost function. Once the travel point is determined, a reference path is evaluated by a risk-based geometric planner. Finally, the reference path is optimized and sent to the UGV.

For the UGV, a LiDAR-based Simultaneous Localization and Mapping (SLAM) algorithm is performed continuously to measure terrain information around its body. The registered point clouds are also fed into a terrain analysis module. Finally, a flexible path is evaluated by a local planner based on the terrain analysis results and the optimized reference path.

For the overall system, the whole active exploration process is executed every time the UAV reaches the current travel point. The entire collaborative system is terminated when the UGV reaches the final target location.

IV. METHODOLOGY

A. Fast Terrain Risk Analysis

Considering that to obtain terrain risk information from sensor measurements in real time is important for our exploration system, a fast terrain risk mapping method is designed and applied to the UAV and the UGV. In our system, we build grid maps for terrain analysis where each grid cell stores elevation information of the point cloud within its area. We use a quadtree data structure for storage and risk analysis of the maps. The leaf node of the quadtree is used to represent the minimum cell in the map, and the area represented by the quadtree is determined by the resolution of the leaf node and the depth of the quadtree. Each quadtree is treated as a ‘block’, and all the ‘blocks’ in the local map are stored through a hash

table, so that any ‘block’ can be quickly indexed and updated by its hash key.

For the UAV, terrain measurements over a large area can be obtained through its wide sensing range. However, due to the long measurement distance, the obtained point clouds contain more uncertainties. Therefore, larger radius and resolution are set to obtain more comprehensive and large-scale terrain information in the mapping process of the UAV. Let m_d^{current} represent the grid map of the UAV. To build the local risk map M_d^{current} , the step height $h_{d,i}$ and slope $s_{d,i}$ of the cell $c_{d,i} \in m_d^{\text{current}}$ are calculated as in [28]. Then, the risk value $r_{d,i}$ of cell $c_{d,i}$ can be calculated by:

$$r_{d,i} = \omega_{d,h} \frac{h_{d,i}}{h_{\text{crit}}} + \omega_{d,s} \frac{s_{d,i}}{s_{\text{crit}}} \quad (1)$$

where h_{crit} and s_{crit} are thresholds that the UGV can endure.

Similarly, the local map is built on the UGV in the same way, but the radius and resolution of the map are set to smaller values to ensure that the UGV can quickly and accurately characterize the terrain information around its body. In this process, the roughness $u_{g,i}$ of each cell $c_{g,i}$ is also calculated and the risk value $r_{g,i}$ of the cell is calculated as:

$$r_{g,i} = \omega_{g,h} \frac{h_{g,i}}{h_{\text{crit}}} + \omega_{g,s} \frac{s_{g,i}}{s_{\text{crit}}} + \omega_{g,u} \frac{u_{g,i}}{u_{\text{crit}}} \quad (2)$$

The weight parameters in (1) and (2) are sum up to 1 separately and are determined empirically according to the traversability of the UGV.

B. Local Target Point Selection

Algorithm 1: Local Target Selection

Input: Previous and current aerial risk maps:
 $M_d^{\text{Previous}}, M_d^{\text{current}}$, Previous target point: \mathbf{v}_{k-1}

Output: Next target point: \mathbf{v}_k

- 1 $\delta M \leftarrow M_d^{\text{current}} \setminus M_d^{\text{Previous}}$
- 2 **for** each block $B_i \in \delta M$ **do**
- 3 $C_i \leftarrow \text{SearchFrontierCells}(B_i)$
- 4 **end**
- 5 $C^{\text{new}} \leftarrow \bigcup C_i$
- 6 $F^{\text{new}} \leftarrow \text{ProcessFrontiers}(C^{\text{new}})$
- 7 **for** each frontier $\mathbf{f}_j \in F^{\text{new}}$ **do**
- 8 **if** $\text{IsReachable}(\mathbf{f}_j, \mathbf{v}_{k-1})$ **then**
- 9 $e_{\mathbf{f}_j} \leftarrow \text{CostCalculation}(\mathbf{f}_j)$
- 10 $F^{\text{all}} \leftarrow \text{push_back}(\mathbf{f}_j)$
- 11 $E \leftarrow \text{push_back}(e_{\mathbf{f}_j})$
- 12 **end**
- 13 **end**
- 14 Select $\mathbf{f}_j \in F^{\text{all}}$ with the smallest $e_{\mathbf{f}_j} \in E$ as \mathbf{v}_k

To meet the needs for long-term exploration task in complex and large-scale unknown off-road environments, local travel point selection from UAV’s risk map is the core of our system, which can effectively reduce time cost and path risk of the UGV. Hence, a risk-inspired target point selection method is proposed as in Algorithm 1. Firstly, inspired by [16], to

improve the time efficiency, the search scope of the target point is limited to the latest incremental area δM of the map (Algorithm 1, lines 1) and δM is marked by the risk mapping step at the interval between two decision steps. Then, we perform a frontier search step on δM to obtain the frontier cells set C^{new} (Algorithm 1, lines 2-6). The function $SearchFrontierCells(\cdot)$ is applied to each ‘block’ by using a Breadth-First-Search (BFS) on the quadtree to find the frontier cells. After that, using the function $ProcessFrontiers(\cdot)$, the frontiers cells are clustered by Euclidean distance and the results are filtered to obtain the current new frontiers set F^{new} .

When the new frontiers set is obtained, we further check whether the frontiers are reachable for the UGV through function $IsReachable(\cdot)$ (Algorithm 1, lines 8), where the reachable ones will be taken as candidates for travel point selection. Considering that the purpose of our research is to find a safe path for the UGV to fast reach the goal point instead of exploring the entire unknown environment, we design a multi-factor cost function to assess each candidate \mathbf{f}_j in equation (3) (Algorithm 1, lines 7-13).

$$e_{\mathbf{f}_j} = \lambda_d \frac{d_j}{\sum_{j=1}^M d_j} + \lambda_h \frac{h_j}{\sum_{j=1}^M h_j} + \lambda_r \frac{r_j}{\sum_{j=1}^M r_j} \quad (3)$$

where $\lambda_d, \lambda_h, \lambda_r$ are tunable parameters and M is the total number of the frontiers. d_j, h_j are move cost, global heuristic cost for the UGV and are defined as follows:

$$d_j = \|\mathbf{f}_j - \mathbf{p}_g^{\text{current}}\|^2 \quad (4)$$

$$h_j = \|\mathbf{f}_j - \mathbf{p}_{\text{end}}\|^2 \quad (5)$$

r_j is the risk cost calculated by the top-view risk map. To ensure that the selected target point is safe enough for the UGV, we calculate a reference path for each candidate. A risk-based geometric planner is executed and the risk values of the local map are introduced into a A* algorithm to calculate the reference path. The path cost $g(i)$ and local heuristic cost $h(i)$ of each cell $c_i \in M_d^{\text{current}}$ are replaced as:

$$g(i) = \sum_{i=0}^{n-1} r_i + \theta \sum_{i=0}^{n-1} \|c_k - c_{k+1}\|^2 \quad (6)$$

$$h(i) = \theta \|c_i - \mathbf{v}_k^{\text{next}}\|^2 \quad (7)$$

where $\|c_k - c_{k+1}\|^2$ is the Euclidean distance between two cells. The shortest Euclidean distance to the travel target point $\mathbf{v}_k^{\text{next}}$ is used as the local heuristic cost and θ is a relative weight parameter between the distance penalty and risk penalty, which is assigned a small value to ensure the path is safe enough. It should be noted that the cell with risk value greater than 0.5 is considered as an obstacle and is non-traversable during geometric path planning.

Thus, the risk cost of each candidate can be calculated as:

$$r_j = \frac{1}{N_j} \sum_{j_s=1}^{N_j} r_{j_s} \quad (8)$$

where r_{j_s} is each cell’s risk value of the reference path and N_j is length of the path. With the cost of each candidate, the frontier with the minimum cost is selected as the next local target point $\mathbf{v}_k^{\text{next}}$ (Algorithm 1, lines 14).

C. Reference Path Optimization

The reference path generated in the previous step may not be directly used for UGV to track. Firstly, due to the long measuring distance of the UAV, uncertainties exist in the local map it captures, resulting in parts of the reference path deviating significantly from the optimal route. In addition, the kinematics of the UGV has not been taken into account, and there may be some turns with large curvatures in the calculation of the reference path. Hence, in order to enhance the efficiency and safety of the exploration process in unknown off-road environments, the reference path is optimized in this step.

First, Bezier curve is applied to smooth the reference path to improve vehicle execution efficiency as follows:

$$B(t) = \sum_{i=0}^{n-1} \binom{n-1}{i} (1-t)^{n-1-i} \cdot t^i \cdot P_i \quad (9)$$

where $P_0, P_1 \dots P_{n-1}$ are the control points extracted from the original reference path. By using Bezier curve, we generate path with good curvature properties and smooth changes to adapt to vehicle kinematics and road conditions, so that the body pose can remain safe and stable. Then, we discretize the smoothed reference path to generate a series of control points and the control points are used as the target point of a local planner [29] on the UGV. The local planner combines the target point and the UGV’s local terrain analysis results to flexibly avoid risks.

V. SIMULATION EXPERIMENTS

To validate the performance of the proposed aerial active exploration system, experiments in simulated environments were conducted. Quantitative and qualitative results are both presented for analysis.

A. Experiment Setup

The simulated experiments were conducted on a personal computer with an Intel Core i7-10700KF CPU @ 3.80GHz, 32 GB RAM and Ubuntu Linux. Gazebo was applied to perform the simulated off-road experiment, where the terrain model was generated by using TerreSculptor¹ to process real remote sensing Digital Elevation Model (DEM) data. The UAV model was an open-source model called *iris* and was equipped with a downward solid-state LiDAR called *Livox-Mid360* for terrain risk mapping. The UGV model was *SCOUT MINI* which was produced by AGILE-X² and carried a 16-line LiDAR for terrain mapping and analysis. The flight altitude of the UAV was set to 8m. The map range and resolution of the UAV were 30m and 0.4m, while those of the UGV were 10m and

¹<https://www.demenzunmedia.com/home/terresculptor/>

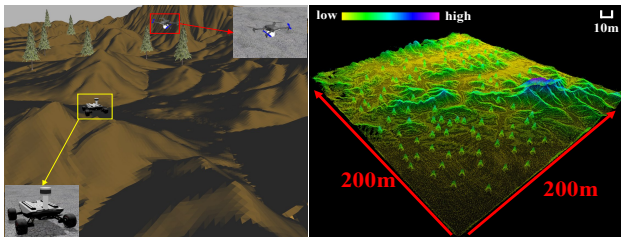
²<https://www.agilex.ai/>

TABLE I
TRAJECTORY CHARACTERISTICS OF THREE SYSTEMS IN DIFFERENT TASKS. THE BEST RESULT IS HIGHLIGHTED IN **BOLD**.

Characteristics		Task 1			Task 2			Task 3		
		Single UGV	w/o risk	UAV-UGV	Single UGV	w/o risk	UAV-UGV	Single UGV	w/o risk	UAV-UGV
Efficiency	Length (m)	338.97	334.47	310.63	233.12	248.57	228.97	214.56	219.52	214.17
	Time (s)	238.71	348.41	196.60	176.61	177.55	132.35	124.74	132.24	125.98
	Curvature (1/m)	2.15	2.23	0.77	4.29	3.14	1.60	1.72	2.11	1.96
Safety	Roll _{var} (rad ²)	0.65	0.42	0.45	0.45	6.16	0.31	0.27	0.31	0.18
	Pitch _{var}	0.91	0.59	0.70	0.69	0.89	0.45	0.42	0.58	0.28
	Total Risk	209.84	195.33	148.61	135.23	114.20	90.45	108.71	101.29	93.10

TABLE II
PARAMETERS USED IN SIMULATION

Parameter	Value	Parameter	Value	Parameter	Value
$\omega_{d,h}$	1/2	λ_d	2.0	$\omega_{g,h}$	1/3
$\omega_{d,s}$	1/2	λ_h	1.0	$\omega_{g,s}$	1/3
θ	0.1	λ_r	4.0	$\omega_{g,u}$	1/3



(a) Sample Image of Models (b) Terrain Point Cloud Model

Fig. 2. Sample image and model of the simulated off-road environment. (a) Sample image of the simulated off-road environment and robot models. (b) The terrain point cloud model where the points are colored by height values.

0.1m. The other parameters used in the simulation experiments are summarized in Table II. The off-road environment model and sample images are shown in Fig. 2. We specifically selected three pairs of start and end points as exploration tasks for performance analysis. We compared the qualitative and quantitative results of three exploration systems. One of them is FAR planner [30], which is an excellent single-vehicle autonomous exploration system at present and is abbreviated as Single UGV. The other two are our system with and without risk inspiration, which are abbreviated as UAV-UGV and UAV-UGV-w/o-risk.

B. Quantitative Analysis

To evaluate the utility of the proposed risk-inspired active exploration system, trajectory characteristics of the different exploration systems in the three tasks are analyzed. The parameters are divided into two types: efficiency and safety. The first type mainly represents the efficiency and consumption of UGV's autonomous driving, including path length, exploration time and path curvature. The second type mainly considers the driving behavior risk, which are the vehicle's pose variances and the total risk of the path. These two types of parameters

can more comprehensively reflect the efficiency and safety of UGV's driving path in the unknown off-road environment.

Table I summarizes the quantitative comparisons of the three systems in different tasks. For efficiency performance, our complete system achieves the best results on all efficiency parameters in Task1 and Task2, which demonstrate that our system can search an effective reference path for the UGV to quickly drive to the end point at low cost. In terms of safety parameters, the total risk of the path obtained by our system is the lowest in all three tasks, and the vehicle attitude stability is also the strongest in Task 2 and Task 3. Moreover, compared with Single UGV, our approach reduces the overall path risk by 26.8%. It can be seen that our risk-inspired active exploration system can help the UGV avoid high-risk areas in unknown off-road environments, reducing the danger of UGV's autonomous driving.

C. Qualitative Analysis

The qualitative exploration results of Single UGV and our system in Task1 are shown in Fig. 3. As can be seen from the figure, due to the limitation of the sensing range, the Single UGV system produced multiple reentries and large turns during the exploration process, which is shown in the green box I. In contrast, the area marked by brown box II show that with the assistance of the UAV, the UGV could reduce unnecessary exploration and avoid getting stuck in a dead end. Moreover, as can be seen from the green box III, the UGV passed through a narrow areas and the driving risk was large. However, in our system, the UGV was guided by the drone to drive on a flatter and safer path, effectively reducing the probability of the UGV to roll over and get trapped.

Fig. 4 shows the exploration results in Task2. Similarly, it can also be learned from the green box I and III that due to the lack of sufficient terrain risk information, single UGV passed through more bumpy terrain during exploration, increasing the driving risk and reducing the exploration efficiency. On the contrary, the proposed risk-inspired aerial active exploration approach can help the UGV drive on flatter areas on the other side, improving its navigation efficiency and reducing its travel cost.

In addition, to generally demonstrate the exploration performance, the path results of the three systems in different tasks are shown in Fig. 5. As can be seen from the comparison

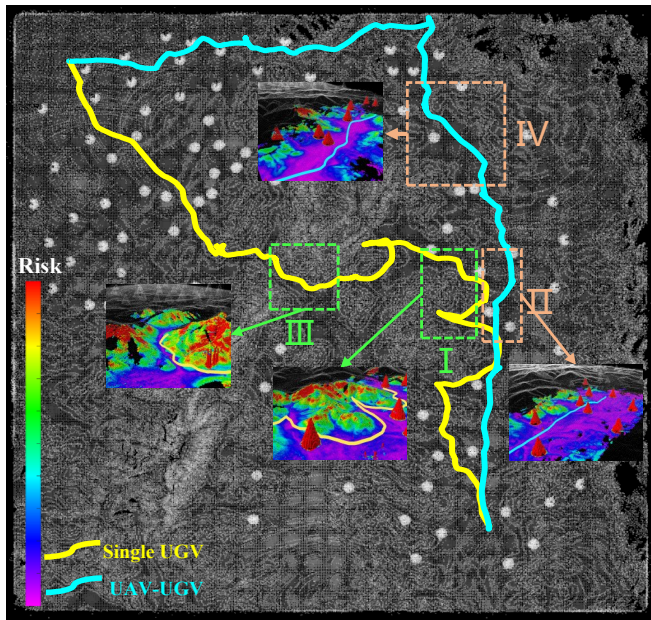


Fig. 3. Qualitative results of Single UGV and UAV-UGV in Task1. Parts of terrain risk information near the driving path are shown in the figure. The areas marked by green boxes belong to Single UGV and those marked by brown boxes belong to UAV-UGV.

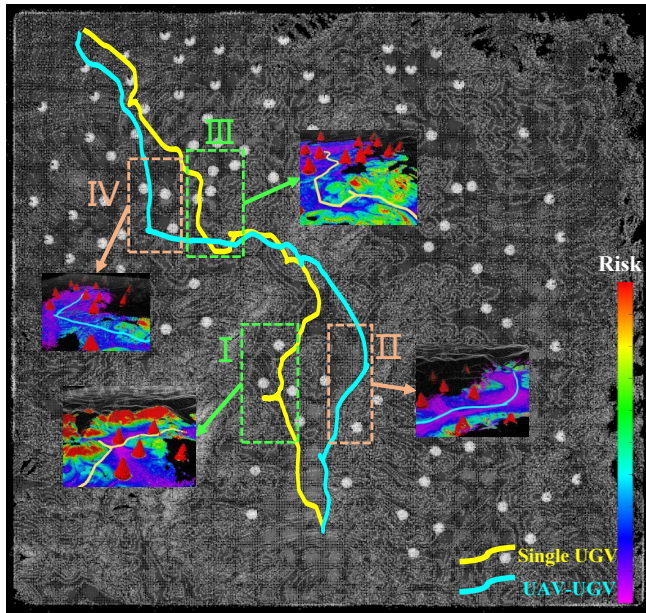


Fig. 4. Qualitative results of Single UGV and UAV-UGV in Task2. Parts of terrain risk information near the driving path are shown in the figure. The areas marked by green boxes belong to Single UGV and those marked by brown boxes belong to UAV-UGV.

results, through terrain risk inspiration, our system can provide smooth, efficient and safe reference path for the UGV in unknown off-road environments.

VI. CONCLUSION

To enhance the autonomous driving of UGV in unknown off-road environments, a risk-inspired aerial active exploration

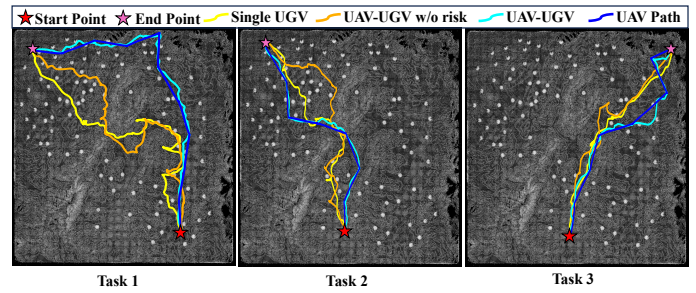


Fig. 5. Qualitative path comparison of three different exploration tasks from top-down view. The UAV path generated by *UAV-UGV* is presented in cyan lines. The other three colored path are the UGV's path generated by different methods.

system is proposed in this paper, which uses a downward solid-state LiDAR on the UAV to extract large-scale terrain risk information and provide reference path for the UGV. Terrain risk information in off-road scenarios has been applied to the exploration process to improve the safety of UGV autonomous driving. The proposed framework was verified by experiments in simulated off-road environments and several different exploration tasks were designed for test. The experiment results demonstrate the effectiveness of the system. In future work, we will further study multi-robot active exploration system and enhance the collaboration ability between the UAV and the UGV in unknown off-road environments.

REFERENCES

- [1] Delmerico, Jeffrey, et al. "The current state and future outlook of rescue robotics." *Journal of Field Robotics* 36.7 (2019): 1171-1191.
- [2] Oh, Hyondong, Seungkeun Kim, and Antonios Tsourdos. "Road-map-assisted standoff tracking of moving ground vehicle using non-linear model predictive control." *IEEE Transactions on Aerospace and Electronic Systems* 51.2 (2015): 975-986.
- [3] Shen, Changsheng, et al. "Collaborative air-ground target searching in complex environments." 2017 IEEE International Symposium on Safety, Security and Rescue Robotics (SSRR). IEEE, 2017.
- [4] Delmerico, Jeffrey, et al. "Active autonomous aerial exploration for ground robot path planning." *IEEE Robotics and Automation Letters* 2.2 (2017): 664-671.
- [5] Miller, Ian D., et al. "Stronger together: Air-ground robotic collaboration using semantics." *IEEE Robotics and Automation Letters* 7.4 (2022): 9643-9650.
- [6] Kulkarni, Mihir, et al. "Autonomous teamed exploration of subterranean environments using legged and aerial robots." 2022 International Conference on Robotics and Automation (ICRA). IEEE, 2022.
- [7] Wang R, Fu M, Wang K, et al. Aerial-Ground Collaborative Continuous Risk Mapping for Autonomous Driving of Unmanned Ground Vehicle in Off-Road Environments[J]. *IEEE Transactions on Aerospace and Electronic Systems*, 2023.
- [8] Zhang, Shiyong, et al. "Fast active aerial exploration for traversable path finding of ground robots in unknown environments." *IEEE Transactions on Instrumentation and Measurement* 71 (2022): 1-13.
- [9] Cao, Chao, et al. "TARE: A Hierarchical Framework for Efficiently Exploring Complex 3D Environments." *Robotics: Science and Systems*. Vol. 5. 2021.
- [10] Dang, Tung, et al. "Graph-based path planning for autonomous robotic exploration in subterranean environments." 2019 IEEE/RSJ International Conference on Intelligent Robots and Systems (IROS). IEEE, 2019.
- [11] Zhang, Xuetao, et al. "A novel informative autonomous exploration strategy with uniform sampling for quadrotors." *IEEE Transactions on Industrial Electronics* 69.12 (2021): 13131-13140.
- [12] Wang, Chaogun, et al. "Efficient autonomous exploration with incrementally built topological map in 3-D environments." *IEEE Transactions on Instrumentation and Measurement* 69.12 (2020): 9853-9865.

- [13] Bircher, Andreas, et al. "Receding horizon" next-best-view" planner for 3d exploration." 2016 IEEE international conference on robotics and automation (ICRA). IEEE, 2016.
- [14] Yamauchi, Brian. "A frontier-based approach for autonomous exploration." Proceedings 1997 IEEE International Symposium on Computational Intelligence in Robotics and Automation CIRA'97.'Towards New Computational Principles for Robotics and Automation'. IEEE, 1997.
- [15] Keidar, Matan, and Gal A. Kaminka. "Efficient frontier detection for robot exploration." The International Journal of Robotics Research 33.2 (2014): 215-236.
- [16] Quin, Phillip, et al. "Expanding wavefront frontier detection: An approach for efficiently detecting frontier cells." Australasian Conference on Robotics and Automation, ACRA. 2014.
- [17] Wang, Chaoqun, et al. "Autonomous robotic exploration by incremental road map construction." IEEE Transactions on Automation Science and Engineering 16.4 (2019): 1720-1731.
- [18] Best, Graeme, et al. "Resilient multi-sensor exploration of multifarious environments with a team of aerial robots." Robotics: Science and Systems (RSS). 2022.
- [19] Bastani, Favyen, et al. "Roadtracer: Automatic extraction of road networks from aerial images." Proceedings of the IEEE conference on computer vision and pattern recognition. 2018.
- [20] Zhou, Lichen, Chuang Zhang, and Ming Wu. "D-LinkNet: LinkNet with pretrained encoder and dilated convolution for high resolution satellite imagery road extraction." Proceedings of the IEEE conference on computer vision and pattern recognition workshops. 2018.
- [21] Manderson, Travis, et al. "Learning to drive off road on smooth terrain in unstructured environments using an on-board camera and sparse aerial images." 2020 IEEE International Conference on Robotics and Automation (ICRA). IEEE, 2020.
- [22] Delmerico, Jeffrey, et al. "'on-the-spot training" for terrain classification in autonomous air-ground collaborative teams." International Symposium on Experimental Robotics. Cham: Springer International Publishing, 2016.
- [23] Rothrock, Brandon, et al. "Spoc: Deep learning-based terrain classification for mars rover missions." AIAA SPACE 2016. 2016. 5539.
- [24] Fankhauser, Péter, et al. "Collaborative navigation for flying and walking robots." 2016 IEEE/RSJ International Conference on Intelligent Robots and Systems (IROS). IEEE, 2016.
- [25] Ren, Yunfan, et al. "ROG-Map: An Efficient Robocentric Occupancy Grid Map for Large-scene and High-resolution LiDAR-based Motion Planning." arXiv preprint arXiv:2302.14819 (2023).
- [26] Christie, Gordon, et al. "Radiation search operations using scene understanding with autonomous UAV and UGV." Journal of Field Robotics 34.8 (2017): 1450-1468.
- [27] Russell, David Jacob, et al. "UAV Mapping with Semantic and Traversability Metrics for Forest Fire Mitigation." ICRA 2022 Workshop in Innovation in Forestry Robotics: Research and Industry Adoption. 2022.
- [28] Chilian, Annett, and Heiko Hirschmüller. "Stereo camera based navigation of mobile robots on rough terrain." 2009 IEEE/RSJ International Conference on Intelligent Robots and Systems. IEEE, 2009.
- [29] Zhang, Ji, et al. "Falco: Fast likelihood-based collision avoidance with extension to human-guided navigation." Journal of Field Robotics 37.8 (2020): 1300-1313.
- [30] Yang, Fan, et al. "FAR planner: Fast, attemptable route planner using dynamic visibility update." 2022 IEEE/RSJ International Conference on Intelligent Robots and Systems (IROS). IEEE, 2022.